Icarus 277 (2016) 73–77

Contents lists available at ScienceDirect

Icarus

journal homepage: www.elsevier.com/locate/icarus

Scale-dependent measurements of meteorite strength: Implications for asteroid fragmentation

Desireé Cotto-Figueroa[a,b,*], Erik Asphaug[a], Laurence A.J. Garvie[a,c], Ashwin Rai[d], Joel Johnston[d], Luke Borkowski[d], Siddhant Datta[c], Aditi Chattopadhyay[d], Melissa A. Morris[a,e]

[a] School of Earth and Space Exploration, Arizona State University, PO Box 876004, Tempe, AZ 85287-6004, USA
[b] Department of Physics and Electronics, University of Puerto Rico at Humacao, Call Box 860, Humacao, PR 00792, USA
[c] Center for Meteorite Studies, Arizona State University, PO Box 876004, Tempe, AZ 85287-6004, USA
[d] School for Engineering of Matter, Transport and Energy, Arizona State University, PO Box 876106, Tempe, AZ 85287, USA
[e] Physics Department, State University of New York, PO Box 2000, Cortland, NY 13045, USA

ARTICLE INFO

Article history:
Received 4 February 2016
Revised 27 April 2016
Accepted 1 May 2016
Available online 9 May 2016

Keywords:
Meteorites
Asteroids
Near-Earth objects
Experimental techniques

ABSTRACT

Measuring the strengths of asteroidal materials is important for developing mitigation strategies for potential Earth impactors and for understanding properties of in situ materials on asteroids during human and robotic exploration. Studies of asteroid disruption and fragmentation have typically used the strengths determined from terrestrial analog materials, although questions have been raised regarding the suitability of these materials. The few published measurements of meteorite strength are typically significantly greater than those estimated from the stratospheric breakup of meter-sized meteoroids. Given the paucity of relevant strength data, the scale-varying strength properties of meteoritic and asteroidal materials are poorly constrained. Based on our uniaxial failure studies of centimeter-sized cubes of a carbonaceous and ordinary chondrite, we develop the first Weibull failure distribution analysis of meteorites. This Weibull distribution projected to meter scales, overlaps the strengths determined from asteroidal airbursts and can be used to predict properties of to the 100 m scale. In addition, our analysis shows that meter-scale boulders on asteroids are significantly weaker than small pieces of meteorites, while large meteorites surviving on Earth are selected by attrition. Further, the common use of terrestrial analog materials to predict scale-dependent strength properties significantly overestimates the strength of meter-sized asteroidal materials and therefore is unlikely well suited for the modeling of asteroid disruption and fragmentation. Given the strength scale-dependence determined for carbonaceous and ordinary chondrite meteorites, our results suggest that boulders of similar composition on asteroids will have compressive strengths significantly less than typical terrestrial rocks.

1. Introduction

Modeling studies of asteroid disruption and fragmentation (Melosh et al., 1992; Benz and Asphaug, 1999) use strength and fracture properties derived from experiments using analog materials such as basalt, granite, or lunar rocks (Durda et al., 2011), even though these are unlikely to be representative of asteroid materials (Flynn and Durda, 2004). Knowledge of in situ strength behavior, at a variety of scales and rates, is important to sample return missions (Berry et al., 2013; Brophy and Murhead, 2013) resource utilization, robotic manipulation, and hazardous asteroid mitigation. Observational and experimental evidence (Melosh et al. 1992; Housen and Holsapple, 1999; Consolmagno and Britt, 1998; Fujiwara et al., 2006) suggests that most ~300-m- to ~30-km-sized asteroids are rubble piles. For example, 25,143 Itokawa, the ~300 m target of the Hayabusa sample return mission (Fujiwara et al., 2006), is dominated by regolith of micron-sized dust to 30-m-sized blocks, with particle diameter following a D^{-3} power law size distribution (Barnouin-Jha et al., 2008), possibly throughout the interior, indicating an ongoing disruption process on small asteroids. But to date there is little understanding of the strength properties in this environment, and whether meteorites found on Earth are characteristic of asteroidal materials. Here we show how material properties extrapolate from cm-scales (of laboratory samples and small gravels on asteroids) to meter-sized objects, the

* Corresponding author at: Department of Physics and Electronics, University of Puerto Rico at Humacao, Call Box 860, Humacao, PR 00792, USA. Tel.: +17878509014.
E-mail address: desiree.cotto@upr.edu (D. Cotto-Figueroa).

http://dx.doi.org/10.1016/j.icarus.2016.05.003
0019-1035/

latter including the multi-meter meteoroids that impact Earth's atmosphere (Popova et al., 2011; Borovička et al. 2015).

There have been relatively few studies of the physical properties of meteorites. Most measurements have been non-destructive such as bulk density, thermal conductivity, and elastic constants (Consolmagno et al., 2008; Ibrahim, 2012). Few measurements of meteorite strength have been undertaken, as the samples have to be crushed. As such catastrophic disruption modeling (Melosh et al., 1992, Benz and Asphaug, 1999) parameters have so far been obtained from studies of terrestrial analogs (e.g., basalt and concrete) or from studies limited to single specimens of meteorites (Durda and Flynn, 1999; Flynn et al., 2005; Durda et al., 2011). The few strength measurements performed (Kimberley and Ramesh, 2011) leave open the question of statistical variation of meteorite strength, and the scale variation relevant to asteroid materials.

In order to provide the data necessary to understand or predict the physical and rheological properties up to hundreds-of-meter scales, we undertook repeated destructive measurements of two representative meteorites: Allende, a CV3 carbonaceous chondrite (a primitive Solar System material), and Tamdakht, an H5 ordinary chondrite (typical of the common asteroids in near-Earth orbit (Binzel et al., 1996)). Both meteorites are observed falls. Tamdakht was observed in 2008 over Morocco while Allende was observed in 1969 over Mexico. Both meteorites were recovered immediately after the falls and have been curated ever since. Neither the Tamdakht nor the Allende meteorites show signs of terrestrial weathering. Suitable pieces of Allende are light grey with abundant chondrules and CAIs (calcium-aluminum-rich inclusions). Tamdakht, with a shock grade of S3, exhibits a heterogeneous structure criss-crossed with shock veins and centimeter-sized regions of white (lower shock) and light grey (more highly shocked) matrix. Chondrules are visible but largely integrated into the matrix through extraterrestrial metamorphism. Quasistatic unconfined compression experiments were conducted on ten and thirteen centimeter-sized cubes of Allende and Tamdakht, respectively. The disrupted fragments are preserved for ongoing analysis, including studies of disruption surface morphology and forthcoming microgravity spaceflight experiments (Asphaug and Thanga, 2014).

2. Materials and methods

We conducted our measurements on ten Allende cubes ranging from 0.7-cm to 4.4-cm and on thirteen Tamdakht cubes ranging from 1- to 3-cm. Elastic wave velocity measurements were performed using a manually controlled Olympus 5077 PR electric pulse generator/receiver which is used to generate and pre-amplify the electric pulse sent to the transducer and also performs bandpass filtering to help clean up scatter noise from the received signal. Pairs of Olympus V-110RM full contact through transmission longitudinal wave transducers and V156-RM full contact normal incidence shear wave transducers were used as the sensor/actuator pair. To decrease the necessary contact pressure required to be applied on the meteorite surface and signal attenuation in between interfaces, an Olympus shear wave coupling fluid was used in between the meteorite surface and the sensor/actuator pair. A National Instrument PI-1042 Digital Acquisition system was used to acquire the signal data on a desktop computer and the National Instrument NIScope software was used as a virtual oscilloscope.

As per the Olympus equipment specifications state, samples may be of any geometry that permits clean pulse/echo measurement of sound transit time through a section on thickness. Ideally this would be a sample at least 1.25 cm thick, with smooth parallel surfaces and a width or diameter greater than the diameter of the transducer being used. However, it is recommended that the samples be at least 0.5 cm thick and therefore measurements were obtained for all samples, except for one Allende cube whose compression test was performed before the sound speed equipment was obtained. Measurements were obtained two to four times per side of the samples to account for any anisotropy. All subsequent data analysis and arrival time calculations were performed using LabView and Matlab.

The Uniaxial compression tests for most of the specimens were performed on an Instron 5985 frame with a 250 kN load cell and compression fixtures comprising of 145 mm diameter radial platens with a maximum rated load of 100 kN. Since the Tamdakht specimens with dimensions greater than 1 cm were expected to take more than 100 kN of load, they were tested on radial platens with a diameter of 165 mm and a maximum rated load of 300 kN. All tests were conducted at room temperature and in displacement control with a displacement rate of 0.25 mm per minute to ensure quasi-static conditions. The GOM ARAMIS 5M, a 3D Digital Image Correlation (DIC) system that enables noncontact measurement of displacement and strain fields is also used. This system is particularly suitable for full field 3D deformation and strain measurements under static and dynamic loading. To prepare the specimen for measurements using the DIC system, a random speckle pattern is applied on the surface of the samples by using an opaque white and black color spray. A stochastic spray pattern is critical in tracking the displacements of the speckled dots, especially in small cubic samples. Strains are thus calculated using the inbuilt Instron extensometer as well as with the DIC system. For those specimens with multiple peaks of failure, the maximum strength was that of the peak with less than two percent change with the initial slope.

The Elastic Modulus E is derived from the sound speed measurements given:

$$E = \frac{V_L^2 \rho (1+\nu)(1-2\nu)}{1-\nu} \tag{1}$$

where ρ is the density, V_L and V_S are the longitudinal and shear wave speeds and ν is the Poisson's ration given by:

$$\nu = \frac{1 - 2\left(\frac{V_S}{V_L}\right)^2}{2 - 2\left(\frac{V_S}{V_L}\right)^2} \tag{2}$$

The Elastic Modulus was also derived directly from the compression measurements. Logarithmic strains in the loading direction were calculated using DIC and the stresses and force readings were obtained from the load cell. A linear model was then fitted to the linear portion of the stress strain curve and the slope of the curve was taken to be the Elastic Modulus in the loading direction. Generally the Elastic Modulus derived from these two different methods is within an eleven percent difference in average except for a few outliers. This ensures that although the specifications of the ultrasonic equipment states that ideally specimens should be greater than 1.25 cm, the recommended dimension of 0.5 cm provides accurate results.

3. Results and discussion

Elastic moduli were measured prior to disruption for each cube (see Table 1), viz., Allende $E = 16.66 \pm 4.72$ GPa and Tamdakht, 21.01 ± 6.57 GPa. During disruption the meteorites showed generally uniform deformation in the axial and lateral direction until lateral deformation caused cracks to grow parallel to the load path. Under loading, the cracks likely began from preexisting heterogeneities that produced stress concentrations and grew with increase in lateral deformation leading to axial separation of the specimen at final failure. Shear banding was not observed, though there was lineation on the fracture surfaces parallel to the axial direction. Under compression, Allende cubes developed several competing cracks at low deformations. At higher deformations a single major crack often led to material failure (see Fig. 1). Tamdakht cubes retained

Table 1
Derived measurements of the Allende (A1-A10) and Tamdakht (T1-T13) cubes.

Sample#	Height (cm)	Width (cm)	Thickness (cm)	Mass (g)	σ^* (MPa)	E^{**} (GPa)	V_L(m/s)	V_S(m/s)	$E^{\dagger}$ (GPa)
A1	0.684	0.702	0.687	0.96	24.7	16.27	2101	1566	12.49
A2	0.717	0.707	0.713	1.069	39.6	17.31	2171	1539	13.94
A3	0.712	0.731	0.721	1.08	31.7	17.46	2261	1615	14.70
A4	0.984	0.962	0.981	2.673	27.6	17.21	2361	1667	16.05
A5	0.973	1.038	0.982	2.88	39.2	27.40	3156	2159	28.70
A6	0.977	1.016	1.051	3.04	36.5	15.66	2267	1630	14.94
A7	1.006	0.986	1.064	3.012	22.5	16.26	2781	1740	20.36
A8	1.694	1.73	1.703	14.56	58.4	7.57	2268	1478	14.41
A9	2.658	2.535	2.585	50.50	32.3	12.77	‡	‡	‡
A10	4.323	4.408	4.394	244.7	41.1	8.17	2262	1476	14.38
T1	1.313	1.285	1.275	7.491	83.6	§	2644	1694	23.02
T2	1.305	1.290	1.260	7.410	120.5	23.31	2624	1606	21.63
T3	1.334	1.284	1.270	7.666	130.7	31.05	3415	1796	29.76
T4	1.297	1.294	1.284	7.635	84.3	21.85	2813	1586	22.58
T5	1.300	1.266	1.252	7.268	186	16.89	2977	2063	31.17
T6	1.300	1.295	1.277	7.314	25.9	9.9	1800	1240	10.97
T7	1.311	1.291	1.265	7.558	247.4	23.07	2742	1946	26.54
T8	1.312	1.284	1.267	7.470	120.5	16.93	2781	1330	16.74
T9	1.964	2.155	2.037	29.93	160.2	12.18	2086	1380	14.69
T10	2.094	1.944	2.151	30.73	76.0	15.90	2140	1350	14.96
T11	2.065	1.949	2.105	29.49	99.6	14.68	1976	1290	13.08
T12	3.104	3.130	3.060	100.37	97.0	19.36	2459	1491	18.15
T13	3.048	3.125	3.027	100.85	183.0	25.57	2983	1938	29.82

‡Sound speed measurements were not obtained.
§DIC data file was corrupted.
* Compressive strength.
** Elastic Modulus derived from compression tests.
† Elastic Modulus derived from sound speed tests.

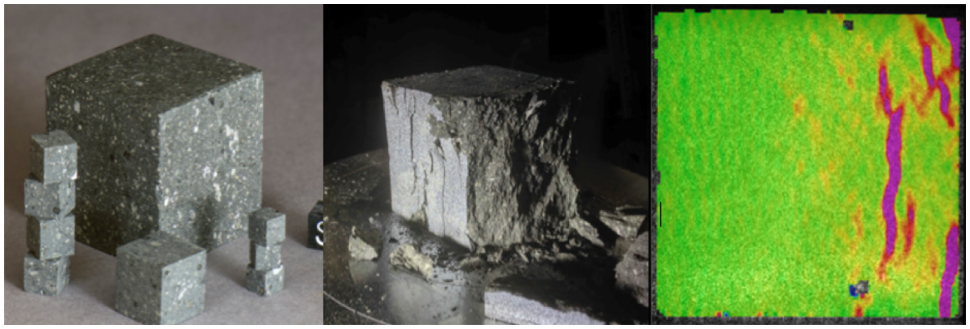

Fig. 1. Examples of Allende cubes, crushed cube, and strain map for one of the crushed cubes. *Left)* Several of the Allende cubes prepared for the compression experiments (0.7 to 4 cm). *Center)* The 4-cm Allende cube after fragmentation. *Right*) False color image showing the strains in the X-direction before failure of the 4-cm Allende cube. Visible are the major cracks (red-magenta) running parallel to the compression direction. (For interpretation of the references to color in this figure legend, the reader is referred to the web version of this article.)

several major cracks even at final failure, leading to finer scale fragmentation. In general, both meteorites suffered brittle material failure similar to low-porosity concrete, with failure in the axial direction and little to no bulging at the cross section (Lawler, 2001; Choi, 1997). These data show that Allende and Tamdakht behave differently under compression.

The meteorites exhibited considerable scatter in their compression strengths (σ): 24.7–58.4 MPa for Allende, and 25.9–247.4 MPa for Tamdakht (see Table 1). The lower scatter in Allende corresponds to its generally more uniform strength properties. Prior to the experiments, we expected that the larger cubes of each meteorite would be weaker than the smaller cubes (Weibull, 1951; Grady and Kipp, 1980), but in fact several of the 1-cm Allende cubes were weaker than the 1.6- to 4-cm specimens. This strength difference may indicate that a 1-cm cube is smaller than the representative volume element (Bazant and Pang, 2007). For example, the Allende cube with the lowest compressive strength contained a 0.5 cm CAI, with a chalky texture that would provide little resistance to deformation and would enhance stress concentration elsewhere in the cube, causing it to fail. Other than chondrules and CAIs, the Allende cubes were free of visible fractures or other structural heterogeneities. In contrast, Tamdakht is crisscrossed by thin shock veins, slickensides and cracks. One of the 3-cm cubes of Tamdakht failed along a slickenside surface. Several cubes broke along such surfaces during cutting and were unusable, biasing the sample to being stronger than average. The range of strengths as a function of size of the meteoritic materials allows for the determination of the material parameters that determine its scale-dependence and for the prediction of its failure threshold.

Here we consider the stochastic variation in strength and what it implies for weakest-link failure of larger random specimens (meteoroids and boulders) of the same material, using a Weibull approach (Weibull, 1951; Wu et al., 2006) common to theoretical studies of asteroid disruption (Melosh et al., 1992; Benz and Asphaug, 1999; Housen and Holsapple, 1999). Allende and Tamdakht showed great variation in uniaxial compressive strength, even when restricted to 1-cm samples, and assuming no bias in cube preparation, this distribution reflects the flaw characteristics in each material.

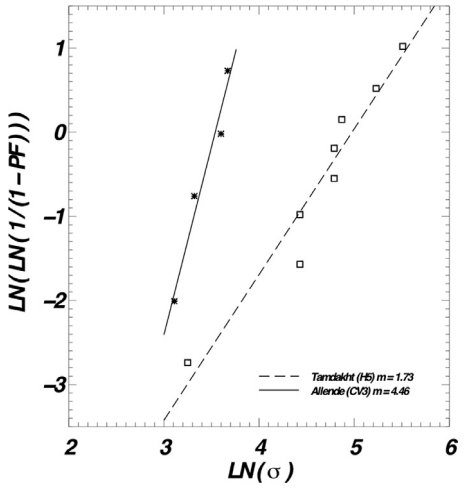

Fig. 2. Plot of cumulative probability of failure versus strength. The horizontal axis indicates the natural log of the strength σ while the vertical axis indicates the double natural log of $1/(1\text{-}P_F)$, where P_F is the probability of failure. Data of the four ~1-cm specimens of Allende and the eight ~1-cm specimens of Tamdakht is shown as asterisks and squares, respectively. The slope of the fitted line to Eq. 4 gives m=4.46±0.06 for Allende and m=1.73±0.06 for Tamdakht.

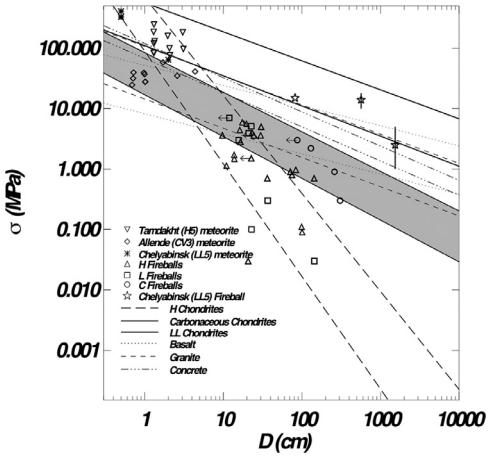

Fig. 3. Strength scale-dependence of meteoritic materials and terrestrial analogs, derived from crush measurements of laboratory specimens. Predicted scale-dependence is extrapolated to data for fireballs. The horizontal axis indicates the diameter D in centimeters and the vertical axis indicates the strength σ in MPa, both in logarithmic scale. Solid (shaded area) and long-dash lines indicate the upper and lower limits of the scale-dependence derived here for the carbonaceous and the ordinary chondrites (H), respectively, with a two-sigma variation (SD) of the Weibull parameter m and the Elastic modulus E. Dotted, dashed and dotted-dashed lines indicate the size-dependent upper and lower limits of basalt, granite and concrete (Asphaug et al., 2002; Pollard, 2005, Gere and Timoshenko, 1997). Obtained measurements of strength from the compression tests of meteorites and estimated values of the bulk strength of H, L, and C chondrites fireballs (Popova et al., 2011; Borovička et al. 2015) are shown as well for comparison. Note that the size dependence of chondrites, derived solely from the compression strengths measurements of the meteorites, encompasses most of the airburst data. Measurements of the estimated values of the bulk strength of the Chelyabinsk fireball and compression tests (Borovička et al. 2015) are shown as well along with the estimated size dependence in bold solid lines.

For samples of identical volume, the characteristic statistical variation of strength is given by

$$P_F = 1 - \exp\left[-\frac{V}{V_o}\left(\frac{\sigma}{\sigma_o}\right)^m\right], \quad (3)$$

where P_F is the failure probability, V is the volume of a specimen subject to uniaxial stress σ, V_o is a representative volume with a characteristic strength σ_o, and the parameter m is a constant characteristic of the material. m is commonly called the Weibull parameter or constant. Concrete, granite and basalt have an m of approximately 5, 6 and 9, respectively. By contrast materials with higher m are relatively homogenous, approaching metallic (uniform) behavior as $m \to \infty$. If we restrict ourselves to specimens of approximately the same volume, $V=V_o \approx 1\,\text{cm}^3$ (that is, the four ~1-cm specimens of Allende, and the eight ~1-cm specimens of Tamdakht) we can derive the Weibull parameter m for each material by fitting:

$$\ln\left[\ln\left(\frac{1}{1-P_F}\right)\right] = m\ ln\sigma - m\ ln\sigma_o. \quad (4)$$

Because the volume dependence goes away in the limit that all volumes are identical, the statistical variation in σ/σ_o is also scale independent (Weibull, 1951; Wu et al., 2006). We rank specimens i=1 to n, where n is the number of samples, in order of increasing crushing strength, and assign a failure probability $P_i = (i\text{-}½)/n$ and solve for m by linear regression (Fig. 2). The slope of the fitted line to Eq. 4 gives m=4.46±0.06 for Allende, which is similar to concrete. For Tamdakht m=1.73±0.06; this low value expresses the great sample heterogeneity caused by the uneven distribution of cracks, shock veins, and slickensides.

Weibull theory assumes that samples of the same size are random representatives from a much larger body, so their strength variations express scale-dependent heterogeneity. In particular, such variations can be used to predict the failure strength of a larger sample of the same solid. Fig. 3 plots the derived upper and lower limits (2-sigma errors) of the strengths of Allende as solid lines (shaded area) and those of Tamdakht as long-dashed lines, where at 1 cm the separation indicates the variation in σ/σ_o seen in the lab, and for larger sizes, and the slope is extrapolated to the predicted failure threshold at that size. For reference, the dotted, dashed and dotted-dashed lines show how the size dependence would compare for basalt, granite and concrete (Asphaug et al., 2002; Pollard, 2005, Gere and Timoshenko, 1997).

Together with this extrapolation of our data we plot meteoroid airburst data (Popova et al., 2011; Borovička et al. 2015) of ordinary and carbonaceous chondrites (Fig. 3) for comparison. Brown et al., 2016 finds no clear variation of the inferred strength and mass of 59 fireballs of meter-sized meteoroids, of which only 11 produced recovered meteorites. Indeed at a first glance the airburst data shown in Fig. 3 appears as a simple scatter. However, it is essential to consider the significant diversity in the material composition of these objects. Evident is the fact that the strength of "C fireballs" with respect to size fits within the upper and lower limits of the scale-dependence derived from our Allende data (solid lines with shaded area), and similarly for the "H and L fireballs" and the Tamdakht strength range (long-dashed lines). Size dependence, derived *solely* from the compression strengths measurements of 1-cm meteorites, encompasses most of the airburst data of the corresponding type, lending credence to the ability of laboratory-scale measurements to provide asteroid-scale relevant physical properties and that there is indeed a strength scale-dependence of meteoritic materials. Although the airburst data is heterogeneous, one trend is curious, that C fireballs generally disrupt at higher pressure than H and L fireballs, e.g., are stronger. Centimeter-sized cubes of Tamdakht are generally stronger, stiffer, and harder than Allende cubes; however some fail at the same peak stress as Allende and others are ten times stronger. This heterogeneity implies that average Tamdakht specimens cross over at meter scales and become weaker than Allende.

The measured strength variations have real-world implications for handling asteroid materials in situ (Berry et al., 2013). For example, the Asteroid Retrieval Mission concept (Brophy and Muirhead, 2013) proposes to extract a ~3–5 m boulder from the

surface of a small asteroid. According to Fig. 3, a 3-m carbonaceous chondrite boulder would have a uniaxial compressive strength of $\sigma = 0.99^{+1.01}_{-0.66}$ MPa, while a 3-m ordinary chondrite (H) would have a strength of $\sigma = 0.016^{+0.050}_{-0.014}$ MPa (2-sigma errors). Boulders on asteroids might be stronger than this, selected by surviving impact comminution. The stress environment on an asteroid is much gentler than on Earth; the base of a 3-m boulder feels a pressure of a few Pa, so weak bodies could easily persist.

4. Conclusions

Meteorites are the strongest pieces of natural space debris that survived an unknown number of past processes (ejection from an asteroid surface, disruption upon entering Earth's atmosphere) that alter the true nature of the material of the original parent bodies. While the meteorites available to us might not be truly representative of the parent bodies due to these selection biases, they provide the best window to a deeper understanding of the fundamental physical and mechanical properties of early Solar System materials and help us place constraints on such properties. Meteorites are structurally heterogeneous at the mm to m scales, making it important to consider their statistical strength variations for understanding asteroid structure and regolith evolution, and for contemplating analog materials for science and exploration concept studies. While the strengths of some terrestrial analog materials overlap some meteorites at centimeter scales (Fig. 3), such overlap is not necessarily the case at meter scales, where terrestrial analogs are typically stronger. The Weibull statistical representation is an ideal and will break down when the fractured rock transitions to granular rubble. However, this representation is applicable to meteorite data at cm-scales to meteoroid airburst data at meter-scales. Indeed a reverse approach can be taken for recorded meteorite falls, where the sizes and stresses associated with the bolide disruption is connected to the size and strength of a typical meteorite fragment. For example, using such an approach for the large 2013 bolide over Russia called Chelyabinsk (an LL5 meteorite) gives m=6.13. Fig. 3 also shows the estimated size dependence of Chelyabinsk (bold solid lines) assuming the elastic modulus of Tamdakht. The implication is that Chelyabinsk meteorites are more homogeneous in strength than Allende, something that can only be validated by repeated compressive failure experiments. This study improves our understanding of the typical asteroid material environment and is a step towards placing fundamental constraints on disruption limits of asteroids in order to issues associated with hazardous asteroid mitigation, resource utilization, and human-robotic exploration (Sagan and Ostro, 1994; Berry et al., 2013; Brophy and Muirhead, 2013).

Acknowledgments

Effort by DCF and EA was supported by NASA Early Stage Innovations Program grant NNX14AB08G. LAJG was supported by NASA Origins of Solar Systems grant NNX11AK58G. The Adaptive Intelligent Materials and Systems Center provided experimental equipment and support of AR, JJ, LB, SD, and AC. MAM was supported by NASA Cosmochemistry grant NNX14AN58G and NASA Emerging Worlds grant NNX15AH62G. We are grateful to D. Scheeres for his ideas and support.

References

Asphaug, E., Thanga, J., 2014. Asteroid regolith mechanics and primary accretion experiments in a cubesat. In: Proceedings of 45th Lunar and Planetary Science Conference.
Asphaug, E., Ryan, E., Zuber, M.T., 2002. Asteroid interiors. In: Bottke Jr., W.F., Cellino, A., Paolicchi, P., Binzel, R.P. (Eds.), Asteroids III. University of Arizona Press, Tucson, pp. 463–484.
Barnouin-Jha, O.S., Cheng, A.F., Mukai, T., Abe, S., Hirata, N., Nakamura, R., et al., 2008. Small-scale topography of 25143 Itokawa from the Hayabusa laser altimeter. Icarus 198, 108–124.
Bazant, Z.P., Pang, S.D., 2007. Activation energy based extreme value statistics and size effect in brittle and quasi-brittle fracture. J. Mech. Phys. Solids 55, 91–134.
Benz, W., Asphaug, E., 1999. Catastrophic disruptions revisited. Icarus 142, 5–20.
Berry, K., Sutter, B., May, A., Williams, K., Barbee, B.W., Beckman, M., et al., 2013. OSIRIS-REx touch-and-go (TAG) mission design and analysis. In: Proceedings of the 36th Annual AAS Guidance and Control Conference.
Binzel, R.P., Bus, S.J., Burbine, T.H., Sunshine, J.M., 1996. Spectral properties of near-Earth asteroids: Evidence for sources of ordinary chondrite meteorites. Science 273, 946–948.
Borovička, J., Spurny, P., Brown, P., 2015. Small Near-Earth asteroids as a source of meteorites. In: Michel, P., et al. (Eds.), Asteroids IV. Univ. of Arizona, Tucson, pp. 257–280.
Brophy, R., Muirhead, B., 2013. Near-Earth asteroid retrieval mission (ARM) Study. In: Proceedings of the 33rd International Electric Propulsion Conference, IEPC-2013–82.
Brown, P., Wiegert, P., Clark, D., Tagliaferri, E., 2016. Orbital and physical characteristics of meter-scale impactors from airburst observations. Icarus 266, 96–111.
Choi, S., Shah, P., 1997. Measurement of deformations on concrete subjected to compression using image correlation. Exp. Mech. 37, 307–313.
Consolmagno, G.J., Britt, D.T., Macke, R.J., 2008. The significance of meteorite density and porosity. Chem. Erde-Geochem 68, 1–29.
Consolmagno, G.J., Britt, D.T., 1998. The density and porosity of meteorites from the Vatican collection. Meteorit. Planet. Sci. 33 (6), 1221–1229.
Durda, D.D., Chapman, C.R., Cintala, M.J., Flynn, G.J., Strait, M.M., Minnick, A., 2011. Experimental determination of the coefficient of restitution for meter-scale granite spheres. Icarus 211, 849–855.
Durda, D.D., Flynn, G.J., 1999. Experimental study of the impact disruption of a porous, inhomogeneous target. Icarus 142, 46–55.
Flynn, G.J., Durda, D.D., Sandel, L.E., Strait, M.M., 2005. Dust production from the hypervelocity impact disruption of hydrated targets. Earth Moon Planets 97, 213–231.
Flynn, G.J., Durda, D.D., 2004. Chemical and mineralogical size segregation in the impact disruption of inhomogeneous, anhydrous meteorites. Planet. Space Sci. 52, 1129–1140.
Fujiwara, A., Kawaguchi, J., Yeomans, D.K., et al., 2006. The rubble-pile asteroid Itokawa as observed by Hayabusa. Science 312, 1330–1334, 5778.
Gere, J.M., Timoshenko, S., 1997. Mechanics of Material, 4th Edition CL Engineering.
Grady, D.E., Kipp, M.E., 1980. Continuum modeling of explosive fracture in oil shale. Int. J. Rock Mech. Min. 17, 147–157.
Housen, K.R., Holsapple, K.A., 1999. Scale effects in strength-dominated collisions of rocky asteroids. Icarus 142, 21–33.
Ibrahim, E.I., 2012. The Elastic Properties of Carbonaceous Chondrites. (M.S. thesis). Department of Geoscience, University of Calgary, p. 177.
Kimberley, J., Ramesh, K.T., 2011. The dynamic strength of an ordinary chondrite. Meteorit. Planet. Sci. 46, 1653–1669.
Lawler, J.S., Keane, D.T., 2001. Measuring three-dimensional damage in concrete under compression. Mater. J. 98, 465–475.
Melosh, H.J., Ryan, E.V., Asphaug, E., 1992. Dynamic fragmentation in impacts: Hydrocode simulation of laboratory impacts. J. Geophys. Res. 97 (E9), 14735.
Pollard, D., Fletcher, R., 2005. Fundamentals of Structural Geology. Cambridge University Press.
Popova, O., Borovička, J., Hartmann, W.K., et al., 2011. Very low strengths of interplanetary meteoroids and small asteroids. Meteorit. Planet. Sci. 46, 1525–1550.
Sagan, C., Ostro, S.J., 1994. Dangers of Asteroid Deflections. Nature 368, 501.
Weibull, W., 1951. A statistical distribution function of wide applicability. J. Appl. Mech. 18, 293–297.
Wu, D., Zhou, J., Li, Y., 2006. Unbiased estimation of Weibull parameters with the linear regression method. J. Europ. Ceramic Soc 26, 1099–1105.